PARTEC 2007

Long-range Forces in Homogeneous Granular Gases

M.-K. Müller and S. Luding

Technische Universiteit Delft, DelftChemTech – Nanostructured Materials, The Netherlands

ABSTRACT

In granular matter, consisting of discrete particles, long-range interactions imply that each of the particles is interacting with all others. For many charged granular materials with Coulomb repulsion or large-scale gravitationally attractive systems, a new hierarchical cell algorithm in combination with multipole expansions of the charge distributions in a Molecular Dynamics environment is developed. This will lead to more efficient modelling concerning the particle numbers and thus give deeper insight and understanding of situations, where long-range forces are dominant. In granular systems with long-range interaction forces and dissipative collisions, both effects can lead to large-scale structure formation, whereas already dissipation alone leads to ever growing clusters. For our three-dimensional mono-charged dissipative homogeneous systems we present the effect of both repulsive and attractive mutual long-range forces and make an attempt to predict the collision frequency and the temperature decay in the system by means of the so-called pseudo-Liouville operator formalism.

1 INTRODUCTION

Treating long-range forces by computer simulations of discrete particles correctly has always been a challenge in various research fields such as protein folding in aqueous solutions, the evolution of star clusters in astrophysics [1] or simply the collision behavior of electrostatically charged particles [7]. Algorithms have been developed, e.g., [2] in order to encounter these highly specialized problems in a computationally effective way and have also been implemented in discrete element methods such as Molecular Dynamics.

In this study, we perform Molecular Dynamics simulations of dilute homogeneous dissipative particle aggregates where particles either mutually repel or attract each other via $1/r$-long-range potentials. As reference, we make use of the inefficient pair-wise summation, i.e., we sum up the forces of all particles acting on the particle of interest. We then compare the reference with results that are obtained by our new hierarchical cell algorithm that is more efficient regarding the computational time expense. Finally, we develop a theory for long-range binary particle interactions that is based on the so-called pseudo-Liouville operator formalism, e.g., [3] and compare it with our simulation results.

2 MOLECULAR DYNAMICS

2.1 "Short" and "Long"-range Forces

We use soft-sphere Molecular Dynamics where within each time step Newton's equations of motion for each particle are solved by the simple Verlet integration method. For this, all currently acting forces on each particle have to be known. During a collision between particles i and j with radii $a_i = a_j = a$, a linear repulsive force and dissipation of kinetic energy in normal direction, $\boldsymbol{n}_{ij} = \boldsymbol{r}_{ij}/r_{ij} = (\boldsymbol{r}_i - \boldsymbol{r}_j)/|\boldsymbol{r}_i - \boldsymbol{r}_j|$, is considered. The loss of kinetic energy at each collision is expressed by the coefficient of normal restitution $r = v_{ij}'^{(n)} / v_{ij}^{(n)}$ that gives the ratio of the relative velocities $v_{ij} = |\boldsymbol{v}_{ij}| = |\boldsymbol{v}_i - \boldsymbol{v}_j|$ in normal direction after (primed) and before (unprimed) the collision. During a time step, on one particle i always long-range forces are acting due to the pair-wise summation,

$$\boldsymbol{F}_i^{(long)} = -Kx^2 \sum_{j=1}^{N-1} \sum_{j=k+1}^{N} \frac{\boldsymbol{n}_{ij}}{r_{ij}^2} \quad , \qquad (1)$$

and, if $r_{ij} < 2a$, short-ranged contact forces as well

$$\boldsymbol{F}_i^{(short)} = k(2a - r_{ij})\boldsymbol{n}_{ij} - \gamma_n(\boldsymbol{v}_{ij} \cdot \boldsymbol{n}_{ij})\boldsymbol{n}_{ij} \quad . \qquad (2)$$

x denotes here either the charge or mass of particles if we deal with an electrostatic or gravitational problem with mono-charged particles of the same mass. According to the spring-dashpot model [4], γ_n is a measure for how much kinetic energy is dissipated at each collision whereas k is the spring constant that defines the stiffness. $K = cG$ defines via c (which is positive for repulsive and negative for attractive forces) the strength of the long-range force, where G denotes a constant.

2.2 Linked Cell Neighborhood Search

Pair-wise summation computes the distances between each of the N particles and all others. The computational time expense then scales with the order of the squared particle number, $O(N^2)$. Particles that are far away from each other will not collide within the following few time steps and therefore need not to be detected for collision. Thus, we can reduce the time expense to $O(NM)$ if we check only M neighboring particles for collision [5]. These particles make up the linked cell neighborhood that consists of all particles

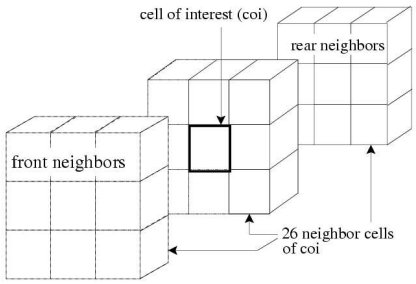

Figure 1: The linked cell neighborhood, including the cell of interest ("*coi*", thick lines) and its 26 directly adjacent neighbor cells (front and rear cells are shifted apart from the other cells).

within the cell of interest ("*coi*") that contains the particle of interest ("*poi*") and of those within its 26 adjacent cells (in 3*D*).

2.3 Hierarchical Linked Cell (HLC) Algorithm

The direct summation of the forces between all particles and the *poi* requires the force computation between all particles and the *poi*. A significant reduction of the number of computations can be achieved if we group far away particles together to pseudo particles. Our HLC algorithm [6] is based on the linked cell structure and combines 27 linked cells to a cell of the hierarchy one level (H1-cell), then 27 H1-cells to a H2-cell of the hierarchy two level, etc., until we have reached the maximum hierarchy level. 26 cells of each hierarchy are arranged around *coi*, changing in size and distance in each hierarchy. Lower hierarchy cells are closer to *coi* than higher hierarchy cells. Effectively, this gives a reduction of computational time and scales like $O(N\log_3 N)$ for any maximum hierarchy level. Due to symmetry reasons, additionally to the HLC structure we have to introduce an inner cut-off sphere around any *poi*. All neighboring particles inside will be considered by pair-wise summation, all particles outside will be combined to pseudo particles according to the HLC algorithm as mentioned above.

The force contribution of a pseudo particle can then be expanded in a Taylor's series where the monopole contribution of one pseudo particle, denoted by α, is

$$\boldsymbol{F}_{i\alpha}^{(long)} = -Kx_i \frac{\boldsymbol{n}_{i\alpha}}{r_{i\alpha}^2} \sum_{j=1}^{n_\alpha} x_j \quad , \qquad (3)$$

where n_α is the number of particles which make up the pseudo particle within a hierarchical cell. Dipole and quadrupole terms can be found in any physics textbook and are not shown here.

If *coi* is located close to the limitations of the simulation volume (see Fig. 2), some hierarchical cells do not fit into the simulation volume anymore. They will be taken from the opposite edge of the simulation volume (shown in Fig. 2 as detached hierarchy cells)

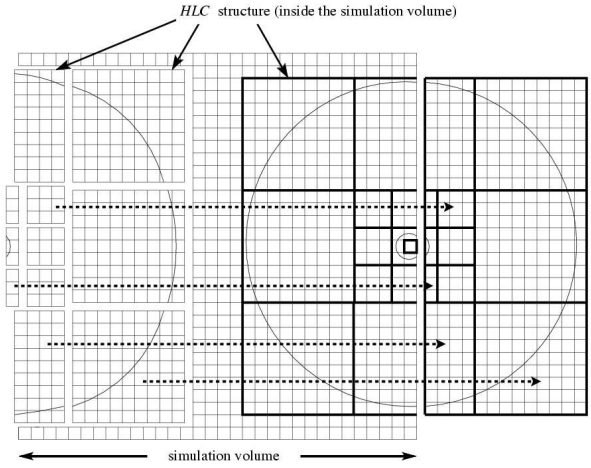

Figure 2: The HLC structure in 2*D* with periodical boundary conditions. Dashed arrows indicate the shift of hierarchical cells to the opposite edge of the simulation volume. For details, see main text.

by shifting them towards the edge where *coi* is located. So, the HLC structure can be completed although parts of it are located outside the simulation volume. This provides for each particle in each linked cell a complete HLC structure, no matter where *coi* is located.

3 RESULTS

3.1 Pseudo-Liouville Operator Theory

For derivation and explanation of the pseudo-Liouville operator formalism, we refer to [3]. Here, we only will outline this idea briefly.

According to classical mechanics, the total time derivative of a dynamical variable, $A(t)$, of a *N*-body system contains the *Hamiltonian* which represents the total energy of the system and its spatial derivatives. Moreover, the system obeys the Liouville-equation that says that during its time evolution all possible states can be taken with same probability, i.e., the probability density in phase space is conserved. For hard sphere systems the interaction potential within the Hamiltonian represents a discontinuous function and problems will arise if we apply spatial derivatives. Therefore, for dissipative hard sphere systems, the pseudo-Liouville operator was introduced in order to bypass these problems and to preserve the formal structure of the Liouville-equation. Although we simulate soft spheres, we can make use of the pseudo-Liouville operator formalism because the soft spheres behave anyway nearly like hard spheres in our simulations besides the effect of strong long range forces. For dynamical variables that are determined by dissipative particle collisions, the interaction part, $\boldsymbol{L}$, of the pseudo-Liouville operator is used for the total time derivative and selects only those pairs of particles that are in physical contact and neglects all others.

The total time derivative expressed by the pseudo-Liouville operator reads

$$\frac{d}{dt}A(t) = \boldsymbol{L}A(t) \qquad (4)$$
$$= \sum_{j=1}^{N-1}\sum_{k=j+1}^{N} |\boldsymbol{v}_{jk}\cdot\boldsymbol{r}_{jk}|\,\Theta(-\boldsymbol{v}_{jk}\cdot\boldsymbol{r}_{jk})\delta(|\boldsymbol{r}_{jk}|-2a)\left(b_{jk}^{+}-1\right)A(t)\,,$$

where j and k are two arbitrary particles. The sums go over all particle pairs. $\delta(|\boldsymbol{r}_{jk}|-2a)$ is the delta function that considers only touching particle pairs, i.e., it vanishes if the distance is larger than twice the radius of the particles. $\Theta(-\boldsymbol{v}_{jk}\cdot\boldsymbol{n}_{jk})$ is the step function that selects only those normal velocities between two particles that are negative, i.e., that lead to an approach and, thus, to a collision between both particles if they are in touch. $|\boldsymbol{v}_{jk}\cdot\boldsymbol{n}_{jk}|$ is the normal component of relative velocity and increases the number of collisions per time unit because higher travel speed will lead to more collisions with other particles. $(b_{jk}^{+}-1)$ is the collision operator that acts on $A(t)$ and changes the velocity and position variables of the particles in $A(t)$ due to the current collision.

Using the collision frequency, $f_E(t) = (2/N)(dC(t)/dt)$, and the (kinetic) energy dissipation rate, $dE_{\mathrm{kin}}(t)/dt$, as dynamical variables in Eq. (4), we apply the concept of ensemble averages by using the N-body distribution function. $C(t)$ is the total number of collisions in the system so far. Skipping all the formal details containing integrations over all phase space coordinates, we only will provide here the solution. Note, that for the velocity integrations we have to distinguish between the presence and absence of long range forces, between repulsive and attractive forces. We obtain for the case without long range potentials

$$f_E^0(t) = 16\sqrt{\pi}na^2g^0(2a)T_g(t)^{1/2} \qquad (5a)$$

$$I^0(t) \equiv \frac{d}{dt}E_{kin}(t) = -8\sqrt{\pi}nNma^2(1-r^2)g^0(2a)T_g(t)^{3/2}\,, \qquad (5b)$$

for the case of long range repulsive potentials

$$f_E(t) = f_E^0(t)\exp\left(-\frac{v_{n,b}^2}{2T_g(t)}\right) \qquad (6a)$$

$$I(t) = I^0(t)\exp\left(-\frac{v_{n,b}^2}{2T_g(t)}\right) \qquad (6b)$$

and for the case of long range attractive potentials

$$f_E(t) = f_E^0(t)\left[2-\exp\left(-\frac{v_{n,e}^2}{2T_g(t)}\right)\right] \qquad (7a)$$

$$I(t) = I^0(t)\left[2-\exp\left(-\frac{v_{n,e}^2}{2T_g(t)}\right)\right]\,. \qquad (7b)$$

Here, $v_{n,b} = (2c_bkx^2/(ma))^{1/2}$ is the critical normal relative velocity both particles have to exceed in order to overcome the repulsion potential barrier and collide. On the other hand, the normal relative velocity has to be less than $v_{n,e} = (2|c_e|kx^2/(ma))^{1/2}$ in order to be caught by the attractive potential and to have a collision. $T_g(t)$ is the granular temperature, m the mass of the mono-dispersed particles, $g^0(2a)$ the pair distribution function for hard spheres at contact that describes the probability to find a neighbour particle exactly at $|\boldsymbol{r}_{jk}| = 2a$ and n denotes the particle number density.

3.1 Simulations including Direct Summation

In order to compare with theory we used the accurate direct summation method. Fig. 3 shows the collision frequency, $f_E(t)$, plotted against the system's temperature for both the repulsive (top) and attractive case (bottom panel) in a double logarithmic plot. $f_E(t)$ decreases because the system cools down due to dissipative collisions (r = 0.85). For different potentials, the simulation results are compared with Eqs. (6a) and (7a). In both cases, for high temperatures in the beginning, the equations and the data approach the classical results, expressed by Eq. (5a) and Haff's law (5b) [9]. For low temperatures, the interaction potential becomes important and deviations from Haff's law occur. For repulsive particles there are also deviations between theory and simulation because theory does not take many body effects into account. In the attractive case, theory indicates pretty well the point when the collision rate increases rapidly and the system becomes strongly inhomogeneous. This corresponds to the hump in $E_{\mathrm{kin}}(t)$ shown in Fig. 4 (bottom) where the particles are close to each other and have higher kinetic energy due to the higher attractive forces. Eqs. (6b) and (7b) are also shown in Fig. 4. Here, due to the many-body effect, theory qualitatively predicts the simulation data, where for high temperatures both theory and data approach the classical result (5a) and (5b) whereas for low temperatures, deviations between $E_{\mathrm{kin}}(t)$ and the classical result occur as well.

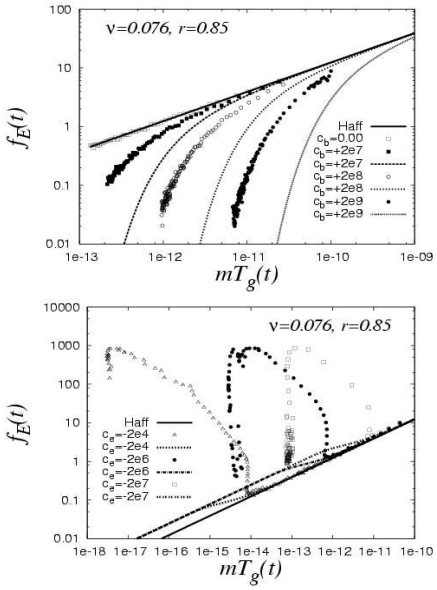

Figure 3: Direct summation method applied for repulsive (top) and attractive systems (bottom). $f_E(t)$ is plotted against temperature for different c_b and c_e.

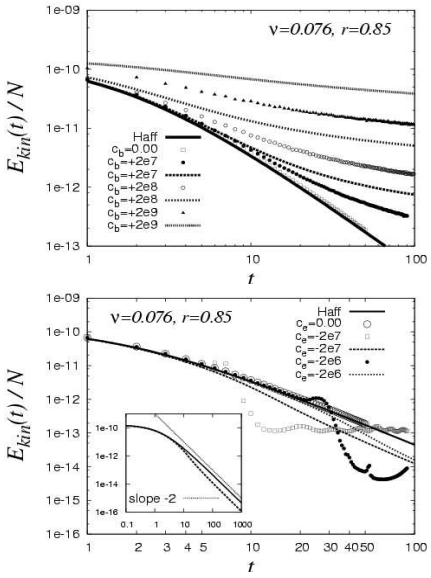

Figure 4: Direct summation method is applied for repulsive (top) and attractive systems (bottom). $E_{\mathrm{kin}}(t)/N$ is plotted against time for different c_b and c_e.

3.2 Simulations including the HLC Algorithm

Fig. 5 shows the results for the same systems as we simulated in Sec. 3.1 but additionally with those obtained by the Hierarchical Linked Cell algorithm. In case of repulsive forces and using the direct summation method, $E_{\mathrm{kin}}(t)$ decreases more than it does in case of HLC. In case of attractive forces, direct summation provides the inhomogeneous regime later than in case of HLC for both c_e = -2·10^7 and -2·10^6. We conclude that the effective potential is slightly increased by the HLC method but shows qualitatively the same results as the direct summation method.

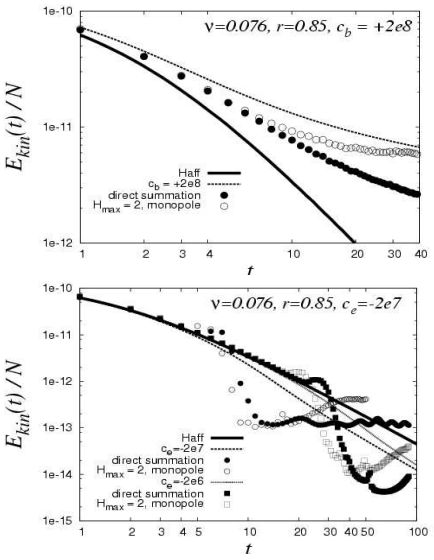

Figure 5: Comparison the HLC algorithm (open symbols) with the direct summation method (solid symbols) for both repulsive forces (top) and attractive forces (bottom). Lines correspond to homogeneous two-particle theory.

4 CONCLUSIONS

We introduced a new algorithm in a Molecular Dynamics environment for 1/*r*-long range forces based on the linked cell structure with periodic boundary conditions and compared it with the results of the accurate direct summation method. For both the repulsive and the attractive case it shows a slightly stronger potential than the direct summation code but is much faster, i.e., it scales like $O(N\log_3 N)$.

Furthermore, we used the pseudo-Liouville operator formalism that is a two-particle theory for hard spheres, extended it for both repulsive and long range interactions and applied it to our simulation results. It turned out that for repulsive forces theory approaches the results found by [7]. For attractive forces it successfully predicts when the transition between the homogeneous and inhomogeneous regime takes place. Additionally, in the limit $T_g(t) >> v^2_{n,b/e}$ it contains the classical results as required.

REFERENCES:

[1] Hut, P., Makino, J., McMillan, S.: Modelling the Evolution of Globular Star Clusters. Nature 336, (1988) p. 31-35

[2] Barnes, J., Hut, P.: A Hierarchical *N*log(*N*) Force Calculation Algorithm. Nature 324, (1986) p. 446-449

[3] Brilliantov, N. V., Pöschel, T.: Kinetic Theory of Granular Gases, Oxford University Press, (2004) p. 127-136

[4] Luding, S.: Collisions & Contacts between two Particles. In: Physics of Dry Granular Media – NATO ASI Series E350. Herrmann, H. J., Hovi, J.-P., Luding, S. (Eds.), Kluwer Academic Publishers, Dordrecht (1998), p. 285

[5] Muth, B., Müller, M.-K., Eberhard, P., Luding, S.: Contacts Between Many Bodies. In: Machine Dynam. Problems. Kurnik, W. (Ed.), (2004) p. 101-114

[6] Müller, M.-K., Luding, S.: Long-range Interactions in Ring-shaped Particle Aggregates. In: Powders & Grains 2005 Stuttgart, Germany. Garcia-Rojo, R., Herrmann, H. J., McNamara, S. (Eds.), Balkema, Leiden, Netherlands (2005), p. 1119-1122

[7] Scheffler, T., Wolf, D. E.: Collision Rates in Charged Granular Gases, Granular Matter 4(3), (2002) p. 103-113

[8] Miller, S. and Luding, S.: Cluster Growth in Two- and Three-dimensional Granular Gases, Phys. Rev. E 69(3), 031305_1-8, 2004

[9] Haff, P. K.: Grain Flow as a Fluid Mechanical Phenomenon, J. Fluid Mech. 134, (1983) p. 401-430